PHYSICAL REVIEW B VOLUME 32, NUMBER 12 15 DECEMBER 1985

Electronic structure and Fermi surface of calcium

P. Blaha and J. Callaway
Department of Physics, Louisiana State University, Baton Rouge, Louisiana 70803
(Received 12 August 1985)

The electronic structure of calcium is calculated by means of the self-consistent linear combination of Gaussian orbitals method and the local-density approximation (LDA). No shape approximations to the charge density or the potential are made. We obtain a band structure and a Fermi surface which is in reasonable agreement with experiment. For that reason we disagree with the conclusions drawn in a recent paper by Jan and Skriver, who employed the linear muffin-tin orbital method and stated that the LDA cannot give a reasonable Fermi surface. Our empty d-band width is somewhat narrower in comparison with other calculations or experiment, as one can also see from our calculated optical conductivity. X-ray form factors, which deviate only slightly from the free-atom values, and Compton profiles, are also given.

I. INTRODUCTION

Although the electronic structure of Ca has been investigated by several authors,[1-11] their conclusions are by no means the same. One might think that a relatively simple metal like Ca, which crystallizes in the fcc structure, would exhibit almost free-electron-like behavior, and be described reliably by many different computational methods or physical models. However, although free-electron-like behavior applies at the bottom of the valence bands, at the top (close to the Fermi energy) hybridization with d states occurs, so that the corresponding Fermi surface (FS) deviates considerably from the free-electron one.

de Haas—van Alphen measurements on single crystals, carried out independently by two groups,[12,13] are in excellent agreement with each other and provide an accurate test of theoretical studies of this simple metal. From these measurements one can determine that the FS consists of a first hole band surface (see, e.g., Fig. 3 of Ref. 8) which is connected at $K=U$ $[(\frac{3}{4},\frac{3}{4},0)(2\pi/a)]$, and second electron band lenses centered at L $[(\frac{1}{2},\frac{1}{2},\frac{1}{2})(2\pi/a)]$.

FS's calculated by various theoretical approaches are not only in quantitative disagreement, but they also predict different shapes. Whereas all calculations find the second-band lenses, many of them do not connect the first hole band surface at K. This orbit is extremely sensitive to the Fermi energy, which is only a few mRy below the eigenvalue at K.

Possible reasons for the failure to predict the correct shape of the first-band FS include the following.

(i) Shape approximations to the potential (muffin-tin, atomic-sphere approximation), as indicated in the work of Perrot,[6] who found non-muffin-tin corrections of the order of ± 4 mRy, which is sufficient to bring his FS into agreement with experiment.

(ii) The choice of particular exchange-correlation potentials. This last observation led to calculations based on the local-density-approximation (LDA), **k**-dependent potentials,[2] Hartree-Fock theory,[5] and semiempirical calculations.[3,9]

One of the most recent calculations employed the Korringa-Kohn-Rostaker (KKR) method with Kohn-Sham exchange,[8] and found a correctly shaped FS. Two other calculations were based on von Barth—Hedin—like potentials and used in the KKR (Ref. 10) and the linear muffin-tin orbital (LMTO) method,[9] respectively. The latter two found a disconnected first hole band FS and the authors of Ref. 9 traced this back to a failure of the LDA. For that reason these authors introduced two empirical potentials in their LMTO calculations (a Gaspar-like potential and an adjusted LDA potential) and found these potentials to be superior to the LDA in describing the FS of Ca as well as structural properties under pressure (semimetal transition, equation of state).

For a clarification of these discrepancies we employed the linear combination of Gaussian orbitals (LCGO) band-structure calculational method,[14] which makes no shape approximations to charge densities or potentials and should therefore be capable of determining whether a correct FS is obtainable in the LDA or if the conclusions drawn in Ref. 9 are valid.

II. COMPUTATIONAL METHOD

The LCGO method has been successfully applied to various metals[15,16] and is described in detail in Ref. 14. Some technical modifications that we have introduced in order to improve accuracy are described below.

In this method one expands the Coulomb as well as the exchange-correlation potential in a Fourier series. The coefficients $V_{xc}(\mathbf{K})$ are obtained in an obvious way by Fourier transformation. For the numerical integration, the unit cell is divided into two parts: touching spheres and an interstitial region (as in muffin-tin-based methods). Inside the spheres, $V_{xc}(\mathbf{r})$ is expanded into Kubic harmonics and integrated accurately by Filon's method (see Eq. 38 in Ref. 14). The integration over the remaining part of the unit cell was done by dividing this space into cubes and integrating over these cubes, assuming a linear variation of $V_{xc}(\mathbf{r})$ inside each cube (Eq. 39 in Ref. 14). The latter approximation gave numerical uncertainties in

$V_{xc}(\mathbf{K})$, especially for large $|K|$.

We have changed the calculation of the interstitial contributions to $V_{xc}(\mathbf{K})$ as follows. We perform a least-squares fit of a Fourier series to $V_{xc}(\mathbf{r})$ in the interstitial region only. This series, whose Fourier coefficients will be denoted $\bar{V}_{xc}(\mathbf{K})$, is rapidly convergent (40—100 stars) and can reproduce the potential in the interstitial region to 6—10 significant digits. We now define a new Fourier series which reproduces the same potential in the interstitial region, but is zero inside the muffin-tin sphere. Let the Fourier coefficients of this series be $V'_{xc}(\mathbf{K})$,

$$V'_{xc}(\mathbf{K})=\Omega^{-1}\int_{\text{int}}\sum_{\mathbf{K}'}\bar{V}_{xc}(\mathbf{K}')\exp[i(\mathbf{K}'-\mathbf{K})\cdot\mathbf{r}]d^3r\ .$$

This integral can be done analytically by subtracting the integral over the spheres from the one over the unit cell instead of by integrating over the interstitial region. This leads to[17]

$$V'_{xc}(\mathbf{K})=\Omega^{-1}\sum_{\mathbf{K}'}\bar{V}_{xc}(\mathbf{K}')\times\begin{cases}\Omega-\dfrac{4\pi}{3}r_m^3\ , & |\mathbf{K}-\mathbf{K}'|=0\\ \Omega-4\pi r_m^2\dfrac{j_1(|\mathbf{K}-\mathbf{K}'|r_m)}{|\mathbf{K}-\mathbf{K}'|}\ , & |\mathbf{K}-\mathbf{K}'|\neq 0\ .\end{cases}$$

In these equations Ω is the volume of the unit cell, r_m is the sphere radius, and j_1 is a spherical Bessel function of $l=1$. The contribution $V'_{xc}(\mathbf{K})$ is added to the results of the numerical integration in the muffin-tin sphere.

In the application to Ca we use a Gaussian-orbital basis as given in Table I and a von Barth—Hedin-like exchange-correlation potential as parametrized by Rajagopal, Singhal, and Kimball.[18] The lattice constant was chosen to be 10.506 a.u. The calculations were carried out to self-consistency using 89 points in $\frac{1}{48}$th of the Brillouin zone and the linear tetrahedron interpolation scheme. The final bands were generated at 505 points and related properties are calculated with this mesh.

III. BAND STRUCTURE AND FERMI SURFACE

Our energy bands, shown in Fig. 1, clearly indicate that the theoretical FS determination depends critically on very fine details. Shifts of a few mRy of the Fermi energy or of the eigenvalues at K or L will create a completely different FS. Some of these crucial eigenvalues are listed in Table II. Our energy for K_1 is 7 mRy higher than the Fermi energy and thus proves that the LDA can predict the correct topology of the first hole band FS, in contradiction to the results of the LMTO calculation, whose authors had to employ empirical potentials in order to get a correctly shaped FS. Cross-sectional areas of our FS are presented in Fig. 2. The second electron band lenses exhibit an almost free-electron-like behavior, while the first holes band surfaces do not.

Table III compares our FS areas with experiment and previous theoretical results. The KKR results[8] with an "exchange-only," $\alpha=\frac{2}{3}$ potential are in better agreement with experiment than ours for two of the four orbits listed in the table; however, we definitely obtain the correct topology of the FS. The errors in the LDA calculation may result from a tendency of this potential to place d bands at too low an energy with respect to s-p bands. This tendency is more pronounced in the LDA than in the $X\alpha$ approximations. The augmented-plane-wave results[4] may suffer from using only six $\mathbf{k}$ points in going to self-consistency.

The LMTO results[9] with a von Barth—Hedin potential show the wrong topology as mentioned above, but with an adjustment of the potential they could fit the experimental FS areas.

TABLE I. Orbital exponents of the Gaussian basis set.

1s	171 384	1p	1000.67	1d	20
2s	25 873	2p	237.31	2d	5
3s	5 984.9	3p	76.4676	3d	1.6
4s	1 712.02	4p	28.7085	4d	0.5
5s	563.304	5p	11.6294	5d	0.18
6s	204.797	6p	4.902 73		
7s	80.418 7	7p	1.921 43		
8s	33.114 5	8p	0.784 693		
9s	9.862 21	9p	0.308 996		
10s	3.977 75	10p	0.134 915		
11s	0.977 055				
12s	0.396 147				
13s	0.065 938				

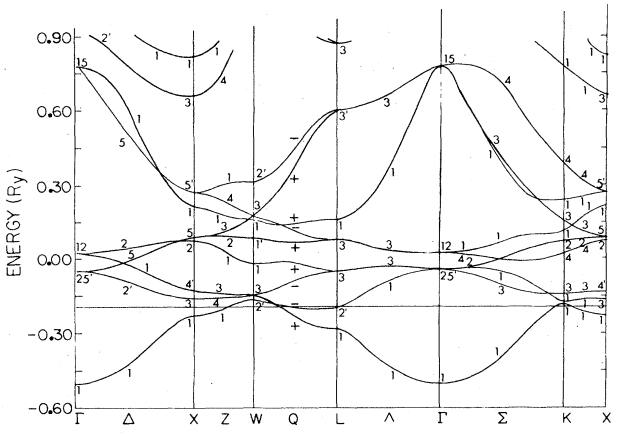

FIG. 1. Energy bands of calcium.

IV. DENSITY OF STATES AND OPTICAL CONDUCTIVITY

The density of states (DOS) is shown in Fig. 3. Free-electron-like behavior can be seen at the bottom of the valence-band DOS, while, closer to E_F, hybridization modifies the free-electron-like DOS. Our valence-band width of 4.2 eV is in reasonable agreement with experiment[19] (3.6±0.2 eV), while the d-band width (4.5 eV) is about 0.5 eV smaller than that of the KKR (Ref. 8) calculation and 1.5 eV smaller than experimental estimates (Ref. 11). We do not find a well-separated, sharp peak at the Fermi energy as other calculations do; however, our DOS at the Fermi energy is nevertheless relatively high, leading to an electronic specific-heat coefficient $\gamma=3.61$ mJ/mol K^2. The experimental values[20–22] range from 1.99 to 3.08 mJ/mol K^2. Because of phonon enhancements one would expect that the theoretical γ should be lower than the experimental one, so that we have here a somewhat unusual situation. On this point, we agree with Jan and Skriver that LDA potentials probably place the d states too low, as mentioned above, and therefore yield a γ larger than experiment.

TABLE II. Eigenvalues at some **k** points in the first Brillouin zone (in rydbergs).

Γ_1	−0.5018	K_1	−0.1838
L_1	−0.2829	K_1	−0.1747
X_1	−0.2280	$W_{2'}$	−0.1641
$L_{2'}$	−0.2002	X_3	−0.1625
E_F	−0.1911	$\Gamma_{25'}$	−0.0466

The optical conductivity shown in Fig. 4 was calculated in standard manner by integration over the Brillouin zone and taking into account the **k** dependence of the momentum matrix elements.[23] It shows a major peak at 4.7–4.8 eV and weaker structure at 3.6–3.7 eV. This two-peak structure was also found in experiment, at 3.7 and 6.0 eV (Refs. 24 and 25) and 4.4 and 5.1 eV (Ref. 26), respectively. The data in the experimental references are presented in graphical form only and cannot easily be presented in our figure. In other theoretical work these peaks were located at 4.5 and 5.2 eV (Ref. 8) and 3.9 and 6.5 eV (Ref. 25). It is difficult to draw firm conclusions from these experimental data, but it is possible that our calculation underestimates the d-band width by about 0.5–1.2 eV. This could be explained as a self-energy effect and approximate treatment of these effects can be achieved with an renormalization factor λ,[23] which is negative in Fe and Ni but positive in Cr and in the present case. One should note that the errors in placement and widths of the d bands in the present case, which are in the range of 10–20%, are much smaller than the percentage errors in the location of excited states relative to occupied ones (the band gap) in covalently bonded semiconductors, these being typically about 50%.

As can be seen from Fig. 4, the onset of the intraband transition does not start at 0 eV, but occurs at about 0.1 eV. This can be traced back to the energy difference of the Q^+ and Q^- states at the Fermi energy, but because of

TABLE III. Comparison of theoretical and experimental Fermi-surface areas. A dash (—) means the orbit was not calculated. (Expt. denotes experimental, Emp. denotes empirical; HF, Hartree-Fock; + C, plus correction; adj., adjusted.)

Name of orbit (center, direction)	Expt. b	Present	KKR c	APW d	Cellular e	Cellular f	Emp. g	HF h	HF + C h	LMTO[a] LDA	LMTO[a] adj.
c or α, W (100)	0.096	0.077	0.095	0.12	0.107	0.125	0.104	0.043	0.049	0.086	0.096
b or β, L (110)	0.129	0.119	0.114	0.05	0.142	0.110	0.116	0.100	0.100	0.066	0.130
a or γ, K (110)	0.024	0.006	0.024	0.01	0.023	0.020	0.024	0.003	i	i	0.023
δ, W (110)	0.096	0.119	—	0.15	—	—	—	0.089	0.093	0.075	0.127

[a]Reference 9.
[b]References 11 and 12.
[c]Reference 8.
[d]Reference 4.
[e]Reference 1.
[f]Reference 2.
[g]Reference 3.
[h]Reference 5.
[i]Orbit does not exist.

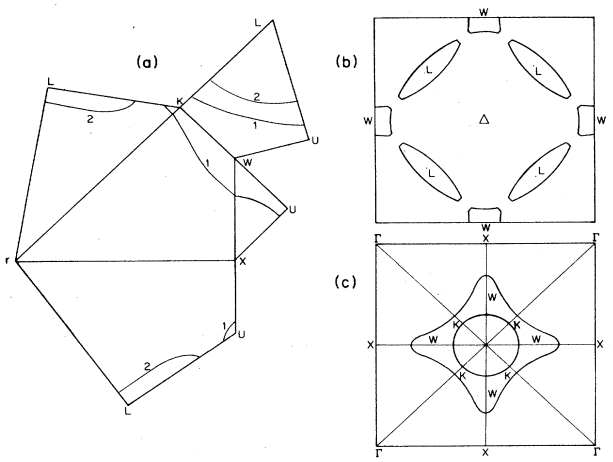

FIG. 2. Fermi-surface profiles of calcium. (a) Unfolded irreducible zone, (b) cross-sectional view perpendicular to the ⟨100⟩ direction at Δ [(0.5,0.5,0.5)(2π/a)], and (c) cross-sectional view perpendicular to the ⟨100⟩ direction at X [(1,0,0)(2π/a)].

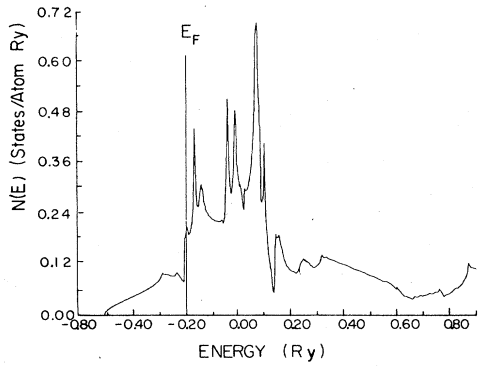

FIG. 3. Density of states of calcium.

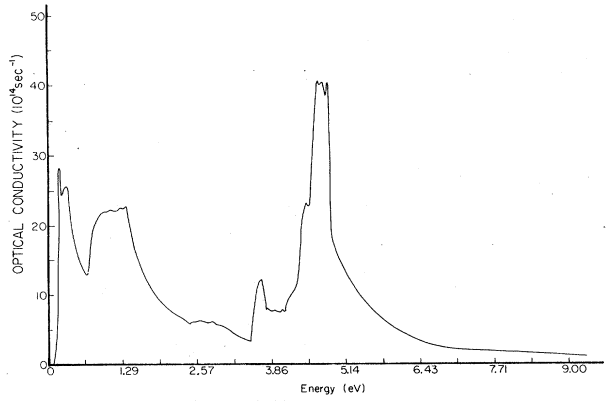

FIG. 4. Optical conductivity of calcium. (A table with numerical data can be obtained from the authors.)

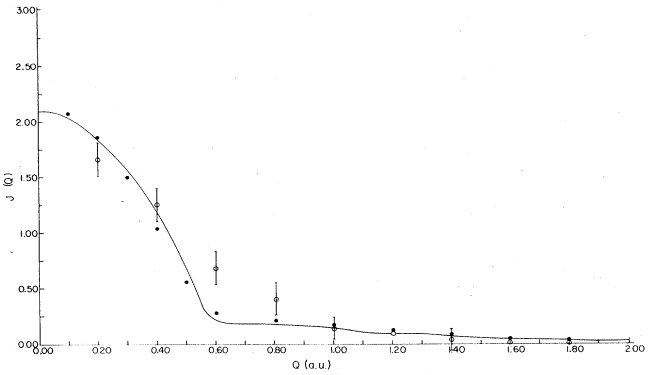

FIG. 5. Spherical averaged Compton profile for calcium (valence contributions only). Solid line, present calculation; open circles, experiment (Ref. 29); dots, Ref. 30.

the Drude conductivity this is unlikely to be observable experimentally.

V. FORM FACTORS AND COMPTON PROFILES

The electronic charge distribution is not very different from that of a simple superposition of free atoms, as can be seen in Table IV, where the x-ray form factors of the free atom (calculated from Hartree-Fock wave functions of Wachters[27]) and of bulk Ca are given. The largest deviation occurs for the (1,1,1) vector and is only about 1%. Nonspherical effects as described by paired reflections [(333) and (511), (422) and (600)] are very small but indicate a slight dominance of e_g symmetry.

The Compton profile, originating from the valence orbitals only, is given in Table V for three different directions; the spherical average is also given. The core contributions can be obtained reliably from Hartree-Fock atomic wave functions.[28] In Fig. 5 the spherically averaged profile is shown together with experimental data[29] and a

TABLE IV. X-ray form factor for calcium.

h	k	l	Atom	Bulk
1	1	1	15.547	15.603
2	0	0	14.857	14.854
2	2	0	12.834	12.831
3	1	1	11.729	11.737
2	2	2	11.415	11.422
4	0	0	10.372	10.381
3	3	1	9.767	9.766
4	2	0	9.592	9.593
4	2	2	8.996	8.995
3	3	3	8.638	8.635
5	1	1	8.638	8.638
4	4	0	8.163	8.159
5	3	1	7.932	7.928
4	4	2	7.863	7.857
6	0	0	7.863	7.859

TABLE V. Compton profile for calcium (only the valence contributions are given).

Q (Ry)	⟨100⟩	⟨110⟩	⟨111⟩	Average	Q (Ry)	⟨100⟩	⟨110⟩	⟨111⟩	Average
0.00	2.199	2.037	2.071	2.092	1.00	0.135	0.143	0.134	0.139
0.05	2.196	2.038	2.062	2.089	1.10	0.108	0.104	0.105	0.106
0.10	2.096	2.007	2.022	2.036	1.20	0.090	0.095	0.080	0.090
0.15	1.987	1.948	1.946	1.959	1.30	0.090	0.084	0.078	0.084
0.20	1.829	1.848	1.846	1.842	1.40	0.078	0.059	0.066	0.066
0.25	1.669	1.733	1.719	1.711	1.50	0.058	0.041	0.049	0.048
0.30	1.512	1.633	1.562	1.580	1.60	0.042	0.038	0.049	0.042
0.35	1.345	1.432	1.394	1.398	1.70	0.028	0.038	0.040	0.036
0.40	1.161	1.200	1.211	1.192	1.80	0.025	0.034	0.029	0.030
0.45	0.948	0.945	1.004	0.963	1.90	0.030	0.024	0.026	0.026
0.50	0.667	0.691	0.693	0.685	2.00	0.026	0.026	0.023	0.025
0.55	0.395	0.409	0.341	0.387	2.20	0.013	0.020	0.011	0.016
0.60	0.224	0.210	0.211	0.214	2.40	0.008	0.008	0.011	0.009
0.65	0.176	0.174	0.215	0.185	2.60	0.011	0.006	0.009	0.008
0.70	0.159	0.177	0.215	0.182	2.80	0.006	0.006	0.007	0.006
0.75	0.166	0.177	0.206	0.182	3.00	0.005	0.010	0.007	0.008
0.80	0.165	0.176	0.187	0.175	3.50	0.003	0.003	0.004	0.003
0.85	0.161	0.173	0.166	0.168	4.00	0.003	0.001	0.003	0.002
0.90	0.154	0.167	0.157	0.161	4.50	0.002	0.003	0.002	0.002
0.95	0.145	0.158	0.147	0.151	5.00	0.001	0.000	0.001	0.001

calculation by Aikala.[30] The agreement with experiment is not overwhelming, but the experimental error bars are very large. Good agreement between the theoretically averaged profiles exists. Aikala[31] has also calculated Compton profiles in the ⟨100⟩, ⟨110⟩, and ⟨111⟩ directions, where he orthogonalized the atomic 4s states on lattice sites neighboring each other, but his results are quite different from ours (especially in the ⟨110⟩ direction) and indicate that a complete description of band-structure and Fermi-surface effects is necessary. To our knowledge no directional Compton-profile measurements are available in the literature for Ca.

VI. CONCLUSION

We have calculated the electronic structure of Ca by the LCGO method and the LDA approximation and have obtained the correct topology of the FS as well as reasonable quantitative agreement with experiment. No empirical potential was necessary to obtain these results. The DOS at the Fermi energy gives a specific-heat coefficient larger than the experimental value. This is unexpected, since, because of electron-phonon enhancements, the experimental value should be larger than theory. The empty d bands are narrower than in experiment, but the general features are reproduced correctly, as can be seen from the optical conductivity. X-ray form factors do not deviate considerably from free-atom values, while for the directional Compton profiles inclusion of band effects is crucial.

ACKNOWLEDGMENT

This work was supported by the Division of Materials Research of the National Science Foundation.

[1]S. L. Altmann, A. R. Harford, and R. G. Blake, J. Phys. F **1**, 791 (1971).
[2]S. L. Altmann, A. R. Harford, and R. G. Blake, J. Phys. F **2**, 1062 (1972).
[3]R. A. Ballinger and B. R. Allen, J. Phys. F **5**, 1135 (1975).
[4]J. W. McCaffrey, J. R. Anderson, and D. A. Papaconstantopoulos, Phys. Rev. B **7**, 674 (1973).
[5]D. J. Mickisch, A. B. Kunz, and S. T. Pantelides, Phys. Rev. B **10**, 1369 (1974).
[6]F. Perrot, Phys. Status Solidi (B) **60**, 223 (1973).
[7]M. Ross and K. Johnson, J. Phys. F **1**, L13 (1971).
[8]C. Lopez-Rios and C. B. Sommers, Phys. Rev. B **12**, 2181 (1975).
[9]J. P. Jan and H. L. Skriver, J. Phys. F **11**, 805 (1981).
[10]V. L. Moruzzi, J. F. Janak, and A. R. Williams, *Calculated Electronic Properties of Metals* (Pergamon, New York, 1978).
[11]P. O. Nilsson, G. Arbman, and D. E. Eastman, Solid State Commun. **12**, 627 (1973).
[12]A. A. Gaertner, J. Low Temp. Phys. **10**, 503 (1973).
[13]R. M. Jenkins and W. R. Datars, Phys. Rev. B **7**, 2269 (1973).
[14]C. S. Wang and J. Callaway, Comput. Phys. Commun. **14**, 327 (1978).
[15]J. Callaway and C. S. Wang, Phys. Rev. B **16**, 2095 (1977).
[16]C. S. Wang and J. Callaway, Phys. Rev. B **15**, 298 (1977).

[17]W. E. Rudge, Phys. Rev. **181**, 1020 (1969).
[18]A. K. Rajagopal, S. P. Singhal, and J. Kimball (unpublished), quoted by A. K. Rajagopal, in *Advances in Chemical Physics,* edited by G. I. Prigogine and S. A. Rice (Wiley, New York, 1979), Vol. 41, p. 59.
[19]L. Ley, G. P. Kerker, and N. Mårtensson, Phys. Rev. B **23**, 2710 (1981).
[20]L. M. Roberts, Proc. Phys. Soc. London, Sect. B **70**, 738 (1957).
[21]M. Griffel, R. W. Vest, and J. F. Smith, J. Chem. Phys. **27**, 1267 (1957).
[22]K. L. Agarwal and J. O. Betterton, J. Low Temp. Phys. **17**, 509 (1974).
[23]D. G. Laurent, J. Callaway, and C. S. Wang, Phys. Rev. B **20**, 1134 (1979).
[24]O. Hunderi, J. Phys. F **6**, 1223 (1976).
[25]P. O. Nilsson and G. Forssel, Phys. Rev. B **16**, 3352 (1977).
[26]J. Marfaing and R. Rivoira, Phys. Rev. B **15**, 745 (1977).
[27]A. J. H. Wachters, J. Chem. Phys. **52**, 1033 (1970).
[28]R. J. Weiss, A. Harvey, and W. C. Phillips, Philos. Mag. **17**, 241 (1968).
[29]R. J. Weiss, Philos. Mag. **28**, 993 (1973).
[30]O. Aikala, Philos. Mag. **31**, 935 (1975).
[31]O. Aikala, Philos. Mag. **32**, 333 (1975).